A gold superatom with 10 electrons in $Au_{13}(PPh_3)_8(p\text{-}SC_6H_4CO_2H)_3$

Shinjiro Takano, Seiji Yamazoe, and Tatsuya Tsukuda

Citation: APL Materials **5**, 053402 (2017); doi: 10.1063/1.4976018
View online: http://dx.doi.org/10.1063/1.4976018
View Table of Contents: http://aip.scitation.org/toc/apm/5/5
Published by the American Institute of Physics

A gold superatom with 10 electrons in $Au_{13}(PPh_3)_8(p\text{-}SC_6H_4CO_2H)_3$

Shinjiro Takano,[1] Seiji Yamazoe,[1,2] and Tatsuya Tsukuda[1,2,a]
[1]*Department of Chemistry, School of Science, The University of Tokyo, 7-3-1 Hongo, Bunkyo-ku, Tokyo 113-0033, Japan*
[2]*Elements Strategy Initiative for Catalysts and Batteries (ESICB), Kyoto University, Katsura, Kyoto 615-8520, Japan*

(Received 14 December 2016; accepted 10 January 2017; published online 13 February 2017)

The title compound $Au_{13}(PPh_3)_8(p\text{-MBA})_3$ (**1**) was synthesized by chemical reduction of the neutral complex $Au(PPh_3)(p\text{-MBA})$(p-MBA = p-$SC_6H_4CO_2H$). Single-crystal X-ray diffraction analysis of **1** showed that the Au_{11} core is protected by seven PPh_3 ligands and an $Au_2(p\text{-MBA})_3(PPh_3)_1$ assembled ligand. Optical spectroscopy indicated that the electronic structure of the Au_{11} core of **1** is significantly different from that of the conventional Au_{11} superatom with an electron configuration of $(1S)^2(1P)^6$. Density-functional theory calculations demonstrated that the Au_{11} core can be viewed as a non-rare-gas-like superatom with an electron configuration of $(1S)^2(1P)^6(1D)^2$. [http://dx.doi.org/10.1063/1.4976018]

Icosahedral Au_{13} clusters and deformed icosahedral Au_{11} clusters can be found as ubiquitous cores in ligand-protected Au clusters as evidenced by single-crystal X-ray diffraction (SCXRD) studies.[1,2] Recent examples of protected Au clusters having Au_{11}/Au_{13} cores are $[Au_{11}(PPh_3)_8Cl_2]^+$,[3] $Au_{11}(PPh_3)_7Cl_3$,[3] $[Au_{13}(PPh_2C_2H_4PPh_2)_5Cl_2]^{3+}$,[4] $[Au_{13}(PPh_2C_2H_4PPh_2)_5(C{\equiv}CPh)_2]^{3+}$,[5] $[Au_{19}(C{\equiv}CPh)_9(PPh_2NHPPh_2)_3]^{2+}$,[6] $[Au_{20}\{P(C_2H_4PPh_2)_3\}_4]^{4+}$,[7,8] and $[Au_{25}(SC_2H_4Ph)_{18}]^-$.[9,10] The high stability of these clusters is associated with both geometric and electronic factors. In these clusters, the Au cores are sterically protected through the passivation of all surface atoms by the ligands via Au–P, Au–Cl, Au–C, and Au–S bonds. The formal number of valence electrons (n^*) confined in the Au_{11}/Au_{13} core is adjusted by the nature of the ligands. A simple electron counting scheme predicts that the n^* value in these Au cores is always eight,[11] forming closed electronic shells with the electron configuration of $(1S)^2(1P)^6$, where 1S and 1P represent superatomic orbitals with angular momenta of 0 and 1, respectively.[11,12] In this regard, the Au_{13}(8e) and Au_{11}(8e) cores in the ligand-protected Au clusters can be viewed as spherical Au superatoms with a rare-gas-like electron configuration.

Synthesis of Au superatoms with non-rare-gas electron configuration is an interesting challenge toward the establishment of a periodic table of artificial elements on a nanoscale.[13,14] Au superatoms with n^* values smaller than 8 have been synthesized by electrochemical and aerobic oxidation, doping with other elements, and deformation of the spherical core into a lower symmetry morphology.[15–25] For example, open electron configuration for Au_{13}(7e) was verified by SQUID[24] and electron paramagnetic resonance (EPR) measurements.[16,21] Closure of two 1P subshells in Au_{13}(6e) and MAu_{12}(6e) (M = Pt and Pd) due to Jahn-Teller distortion was illustrated by voltammetric measurement and density functional theory (DFT) calculation.[23,24] However, to the best of our knowledge, Au_{11}/Au_{13} superatoms with n^* values larger than 8 have not been synthesized up to now.

A new idea or strategy for synthesis is required for the development of a new type of non-rare-gas-like Au_{11}/Au_{13} superatom with $n^* > 8$. In general, the n^* value in the Au core is determined by several factors, such as the size of clusters, the number and nature of the ligands, and the total

[a]Author to whom correspondence should be addressed. Electronic mail: tsukuda@chem.s.u-tokyo.ac.jp

charge of the clusters.[11] In the conventional synthesis, Au_{11}/Au_{13} superatoms prefer to take $n^* = 8$ by adjusting the total charge of the clusters in the presence of free ions in the synthetic system, such as halides, NO_3^-, PPh_4^+, and TOA^+ (TOA = tetraoctylammonium). Thus, we can expect that Au_{11}/Au_{13} superatoms having non-rare-gas-like electron configurations will be obtained by fixing (defining) the charge state of the clusters to neutral in the absence of free ions. In this paper, we report the first synthesis of the Au_{11} superatom with 10 electrons based on this synthetic strategy.

Details of the synthesis of the title compounds and the crystallization procedure are given in the supplementary material. In brief, a neutral Au(I) complex, $Au(PPh_3)$(*p*-MBA) (*p*-MBA = *p*-$SC_6H_4CO_2H$),[26] was used as a precursor of the title compound. First, $Au(PPh_3)$(*p*-MBA) was dispersed in ethanol at 0 °C and then a freshly prepared aqueous solution of $NaBH_4$ (0.5 eq.) was added to this solution at once. The mixed solution was stirred for 2 h at 0 °C and then filtered. The filtrate was evaporated to dryness. After washing the residue with dichloromethane, acetone, and water, the cluster was extracted with ethanol. Slow diffusion of *n*-pentane vapor into the ethanol-DMF dispersion of the crude clusters produced dark-red platelet crystals of **1** after a few weeks (Figure S1 of the supplementary material). Clear ruby-red prism crystals of **2** were obtained when the diffusion rate of *n*-pentane vapor was fast (Figure S1).

Figures 1(a) and 1(b) show the crystal structures of clusters **1** and **2**, respectively, determined by SCXRD analysis. The charge state of **1** was assigned as neutral based on the fact that the lattice volumes of the crystals prepared in the presence and absence of PF_6^- did not change appreciably

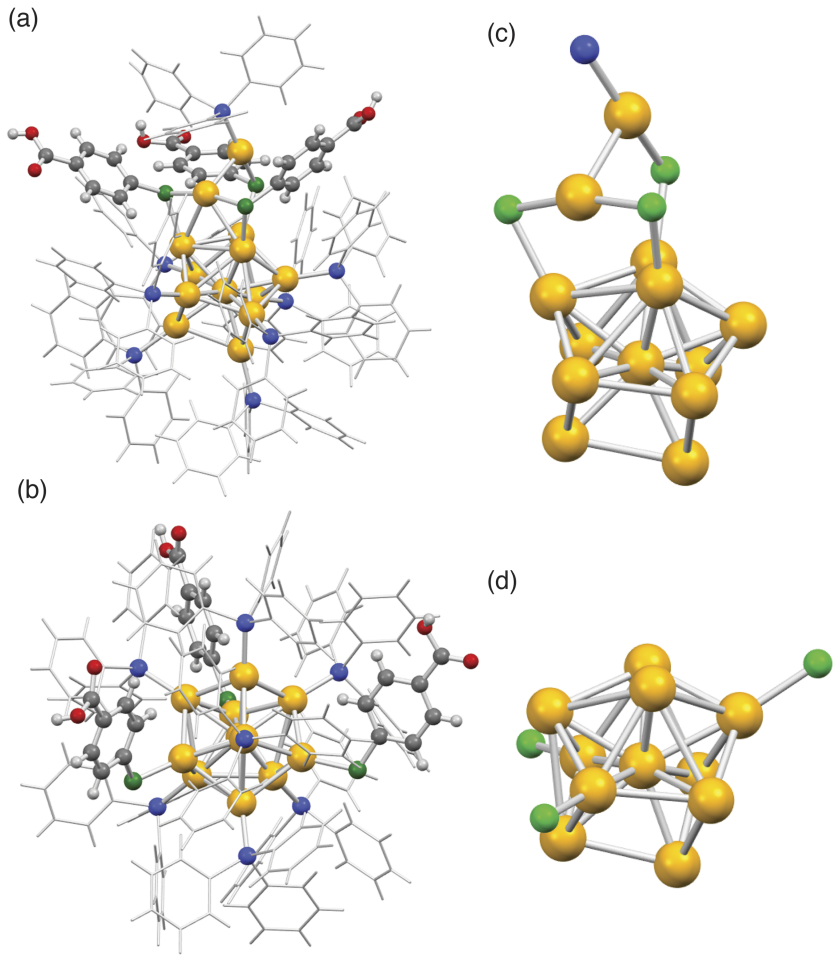

FIG. 1. Single-crystal X-ray structures of (a) **1** and (b) **2**. Phenyl rings of PPh_3 molecules are depicted as sticks. Solvent molecules and disordered atoms are omitted for clarity. Bonding structures of Au and S atoms for (c) **1** and (d) **2**. Color codes: yellow: gold; green: sulfur; blue: phosphorus; gray: carbon; light gray: hydrogen; red: oxygen.

(16 780(80) and 16 807(2) Å^3, respectively). The molecular formulae of **1** and **2** were determined to be $Au_{13}(PPh_3)_8(p\text{-MBA})_3$ and $Au_{11}(PPh_3)_7(p\text{-MBA})_3$, respectively. The composition of **1** was also confirmed by thermogravimetric (TG) analysis: the weight loss experimentally observed (50.3 wt. %) agreed well with the organic moiety calculated for $Au_{13}(PPh_3)_8(p\text{-MBA})_3$ (50.0 wt. %) (Figure S2 of the supplementary material). Ion signals corresponding to $[Au_{13}(PPh_3)_8(p\text{-MBA})_3]^{2+}$ together with small fragments were observed by electrospray ionization mass spectrometry only at spray voltages (>4 kV) significantly higher than those typically applied for ionic Au clusters such as $[Au_{11}(PPh_3)_8Cl_2]^+$ and $[Au_{25}(SC_2H_4Ph)_{18}]^-$ (Figure S3 of the supplementary material). Figures 1(c) and 1(d) compare the core structures of **1** and **2**. Contrary to the expectation based on the composition that **1** has an icosahedral Au_{13} core, the Au_{13} core is composed of subunits of Au_{11} and Au_2. In contrast, **2** has a structure similar to that of $Au_{11}(PPh_3)_7(SPy)_3$ (SPy = 4-mercaptopyridine) reported previosuly.[27] Both the Au_{11} unit of **1** and the Au_{11} core of **2** take the well-known tetra-capped centered chair motif,[1,3] although close inspection showed that they are slightly distorted (Figure S4 of the supplementary material). Three *p*-MBA ligands are directly coordinated to Au_{11} in both **1** and **2** without forming the semi-ring motif –SR–(Au–SR–)$_n$ (n = 1–3) conventionally found in the thiolate-protected Au clusters.[2] However, the bonding configurations are remarkably different between **1** and **2**: three thiolates are ligated to the three Au atoms on a single facet of the Au_{11} unit in **1**, whereas they occupy the equatorial positions of the Au_{11} core in **2**. The Au_2 unit in **1** glued three thiolates bound on the facet. Partial electron transfer from the Au_2 unit to the thiolates may have occurred in **1** judging from the fact that the Au–Au bond length of the Au_2 unit (2.994 Å) is slightly shorter than the aurophilic Au(I)–Au(I) bond in the crystal of $Au(PPh_3)(p\text{-MBA})$ (3.076 Å),[26] but is significantly longer than those typically observed in Au clusters (2.8–2.9 Å).[1,2] It appears that one of the Au atoms in the Au_2 unit forms the –SR–Au–SR– staple motif (Figure 1(c)). However, the geometric structure is distorted significantly as compared with that of the conventional –SR–Au–SR– motif because of the large difference in the distances between two anchoring Au atoms on the core.

The n^* value of **1** is calculated to be 10 given that the individual Au atom provides one electron and the thiolate takes one electron.[11] Based on the unique core structure of **1** (Figure 1(c)), there are two scenarios to explain the electronic structure. The first one is that 10 electrons are confined within the Au_{11} core, whereas the second one assumes that 10 electrons are divided into the two closed electronic structures, Au_{11}(8e) and Au_2(2e). In order to clarify this issue, we conducted DFT calculation on the model system $Au_{13}(P(CH_3)_3)_8(SCH_3)_3$. Since full geometry optimization is not trivial, we focused on the energy levels and shapes of the molecular orbitals of $Au_{13}(P(CH_3)_3)_8(SCH_3)_3$ by fixing the positions of Au, P, and S atoms at those found in the single crystal of **1**. We only considered a singlet spin state based on the results of ESR measurement on **1**: no signal was observed in our preliminary

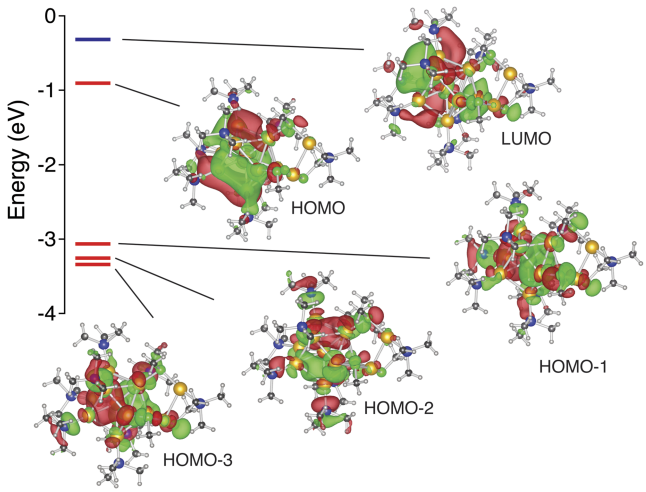

FIG. 2. Energy diagram and Kohn-Sham orbitals of $Au_{13}(P(CH_3)_3)_8(SCH_3)_3$ model cluster near the frontier energy levels. The orbitals are illustrated at the 0.02e level. The color code of the model is the same as in Fig. 1.

measurements at <4 K. Figure 2 shows the energy levels and shapes of the frontier molecular orbitals. Based on the shape of the orbitals, HOMO and LUMO can be assigned to 1D orbitals and HOMO-1 to −3 to 1P orbitals. Importantly, these frontier orbitals are not distributed to the Au_2 unit, but are localized within the Au_{11} unit. This result leads us to conclude that **1** can be viewed as the Au_{11} superatom having 10 electrons with the electron configuration of $(1S)^2(1P)^6(1D)^2$. To the best of our knowledge, this is the first example of the 10e Au superatom. Only one electron is removed from the Au_{11} core although it is bound by three thiolates. This is because the Au_2 moiety, acting as a glue of the three thiolates, reduces the electron withdrawing ability of the three thiolates. In other words, the $Au_2(p\text{-MBA})_3(PPh_3)_1$ moiety can be viewed as a tridentate ligand that can take one electron from the Au_{11} core. It is interesting to note that the 10e Au superatom prefers a singlet state to a triplet state, which is against the trend expected by Hund's rule for conventional atoms. The preference of a singlet state is ascribed to the splitting of 1D orbitals due to the reduced symmetry of the Au_{11} core. Similarly, Jahn-Teller distortion of the Au_{13}(6e) and MAu_{12}(6e) (M = Pt and Pd) structures induces the splitting of triply degenerated 1P superatomic orbitals and two of the 1P orbitals thus stabilized accommodate 4 electrons to form a singlet state.[23,24] These results suggest that Hund's rule cannot be applied in the construction of the periodic table of superatoms because of the structural fluxionality.

Figure 3(a) compares the optical absorption spectra of **1**, **2**, and $Au_{11}(PPh_3)_7(SPy)_3$ having the Au_{11}(10e), Au_{11}(8e), and Au_{11}(8e) cores, respectively. As expected, the spectral profiles of **2** and $Au_{11}(PPh_3)_7(SPy)_3$ are similar, consistent with the fact that both systems have an Au_{11}(8e) core. The slight difference in the spectral profile is probably due to the electronic nature of the SPy and *p*-MBA ligands. On the other hand, the spectrum of **1** exhibits a significantly different profile from those of the 8e superatoms: the optical onset is red-shifted and the profile is smoother. Although assignment of the optical spectrum is beyond the scope of this study, these observations are direct evidence of the difference in the electronic structures of Au_{11} superatomic cores between **1** and **2**. Cluster **1** in EtOH/MeOH(1:1) glass at 77 K showed photoluminescence at 765 nm (1.62 eV) upon photoexcitation in the wavelength range of 300–570 nm (Figure 3(b)). This observation suggests that the photoluminescence is governed by the same electronic transition regardless of the photoexcitation

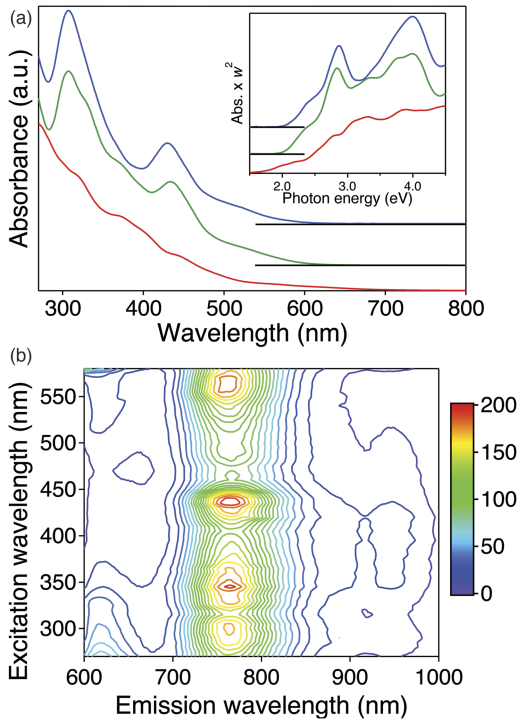

FIG. 3. (a) UV-Vis absorption spectra of **1** (red), **2** (green), and $Au_{11}(PPh_3)_7(SPy)_3$ (blue). The inset shows the same spectra on the energy scale. (b) A contour map of photoluminescence of **1** at 77 K.

mode. Most probably, the photoluminescence is associated with the electronic transition from HOMO (1D) to HOMO-1 (1P) from which an electron is photoexcited into LUMOs (1D). Namely, the energy gap between the highest 1P and lowest 1D superatomic orbitals in **1** is estimated to be 1.62 eV.

In summary, the Au_{11}(10e) superatom with an electron configuration of $(1S)^2(1P)^6(1D)^2$ was synthesized for the first time by chemical reduction of a halogen-free Au(I) precursor. SCXRD and DFT calculation showed that $Au_{13}(PPh_3)_8(p\text{-MBA})_3$ can be viewed as an Au_{11}(10e) superatomic core protected by seven PPh_3 ligands and the assembled tridentate ligand $Au_2(p\text{-MBA})_3(PPh_3)_1$. The non-rare-gas-like electron configuration of the Au_{11} core was supported by optical spectroscopy. Preliminary ESR measurement and photoluminescence spectroscopy suggested that the Au_{11} core is in the singlet state by accommodating two electrons in a 1D superatomic orbital located higher in energy than 1P by 1.62 eV. This study presents the possibility that superatoms with unique electron configurations can be synthesized in the absence of free ions.

See supplementary material for details of the synthesis, characterization, and additional figures.

We thank Professor Toshikazu Nakamura (Institute for Molecular Science, Japan) for his valuable assistance with ESR measurements. This research was financially supported by the Elements Strategy Initiative for Catalysts and Batteries (ESICB) and by the "Nanotechnology Platform" (No. 12024046) from the Ministry of Education, Culture, Sports, Science, and Technology (MEXT) of Japan and a Grant-in-Aid for Scientific Research (A) (Grant No. JP26248003) from the Japan Society for the Promotion of Science (JSPS). S.T. is grateful for the JSPS Research Fellowship for Young Scientists.

[1] D. M. P. Mingos, *Gold Clusters, Colloids and Nanoparticles* (Springer International Publishing, Switzerland, 2014).
[2] T. Tsukuda and H. Häkkinen, *Protected Metal Clusters: From Fundamentals to Applications* (Elsevier, Amsterdam, 2015).
[3] L. C. McKenzie, T. O. Zaikova, and J. E. Hutchison, J. Am. Chem. Soc. **136**, 13426 (2014).
[4] Y. Shichibu and K. Konishi, Small **6**, 1216 (2010).
[5] M. Sugiuchi, Y. Shichibu, T. Nakanishi, Y. Hasegawa, and K. Konishi, Chem. Commun. **51**, 13519 (2015).
[6] X.-K. Wan, Q. Tang, S.-F. Yuan, D.-E. Jiang, and Q.-M. Wang, J. Am. Chem. Soc. **137**, 652 (2015).
[7] X.-K. Wan, S.-F. Yuan, Z.-W. Lin, and Q.-M. Wang, Angew. Chem., Int. Ed. **53**, 2923 (2014).
[8] J. Chen, Q.-F. Zhang, P. G. Williard, and L.-S. Wang, Inorg. Chem. **53**, 3932 (2014).
[9] M. W. Heaven, A. Dass, P. S. White, K. M. Holt, and R. W. Murray, J. Am. Chem. Soc. **130**, 3754 (2008).
[10] M. Zhu, C. M. Aikens, F. J. Hollander, G. C. Schatz, and R. Jin, J. Am. Chem. Soc. **130**, 5883 (2008).
[11] M. Walter, J. Akola, O. Lopez-Acevedo, P. D. Jadzinsky, G. Calero, C. J. Ackerson, R. L. Whetten, H. Grönbeck, and H. Häkkinen, Proc. Natl. Acad. Sci. U. S. A. **105**, 9157 (2008).
[12] J. Akola, M. Walter, R. L. Whetten, H. Häkkinen, and H. Grönbeck, J. Am. Chem. Soc. **130**, 3756 (2008).
[13] P. Jena, J. Phys. Chem. Lett. **4**, 1432 (2013).
[14] Z. Luo and A. W. Castleman, Acc. Chem. Res. **47**, 2931 (2014).
[15] M. Zhu, W. T. Eckenhoff, T. Pintauer, and R. Jin, J. Phys. Chem. C **112**, 14221 (2008).
[16] M. Zhu, C. M. Aikens, M. P. Hendrich, R. Gupta, H. Qian, G. C. Schatz, and R. Jin, J. Am. Chem. Soc. **131**, 2490 (2009).
[17] Y. Negishi, W. Kurashige, Y. Niihori, T. Iwasa, and K. Nobusada, Phys. Chem. Chem. Phys. **12**, 6219 (2010).
[18] Y. Kamei, Y. Shichibu, and K. Konishi, Angew. Chem., Int. Ed. **50**, 7442 (2011).
[19] M. A. Tofanelli and C. J. Ackerson, J. Am. Chem. Soc. **134**, 16937 (2012).
[20] K. Kwak and D. Lee, J. Phys. Chem. Lett. **3**, 2476 (2012).
[21] S. Antonello, N. V. Perera, M. Ruzzi, J. A. Gascón, and F. Maran, J. Am. Chem. Soc. **135**, 15585 (2013).
[22] Y. Negishi, W. Kurashige, Y. Kobayashi, S. Yamazoe, N. Kojima, M. Seto, and T. Tsukuda, J. Phys. Chem. Lett. **4**, 3579 (2013).
[23] K. Kwak, Q. Tang, M. Kim, D. -e. Jiang, and D. Lee, J. Am. Chem. Soc. **137**, 10833 (2015).
[24] M. A. Tofanelli, K. Salorinne, T. W. Ni, S. Malola, B. Newell, B. Phillips, H. Häkkinen, and C. J. Ackerson, Chem. Sci. **7**, 1882 (2016).
[25] M. A. Tofanelli, T. W. Ni, B. D. Phillips, and C. J. Ackerson, Inorg. Chem. **55**, 999 (2016).
[26] J. D. E. T. Wilton-Ely, A. Schier, N. W. Mitzel, and H. Schmidbaur, J. Chem. Soc., Dalton Trans. 1058 (2001).
[27] K. Nunokawa, S. Onaka, M. Ito, M. Horibe, T. Yonezawa, H. Nishihara, T. Ozeki, H. Chiba, S. Watase, and M. Nakamoto, J. Organomet. Chem. **691**, 638 (2006).